Diurnal asymmetry in the GERB(-like) SW fluxes

Cédric Bertrand

Royal Meteorological Institute of Belgium,
Brussels, Belgium.
Cedric.Bertrand@oma.be

5th CERES-II Science Team Meeting/Angular Modeling Working Group Session
Crowne Plaza at Fort Magruder, Williamsburg VA, May 3, 2006

Concern

- Preliminary data from the GERB instrument exhibit systematic asymmetry in the SW flux diurnal evolution

- Such asymmetries are not found in the CERES-TRMM BB SW ADMs used to convert the directional BB GERB SW radiances to fluxes

Monthly mean clear sky SW flux difference at l.n. ± 2 hours (April 04)

Local noon (l.n.)
⇒time of Min(SZA)
on a 15-minutes
slot basis

HIGH RESOLUTION
(3x3 SEVIRI PIXEL)

(A) Clear Sky GERB (G3) SW Flux Morning Difference

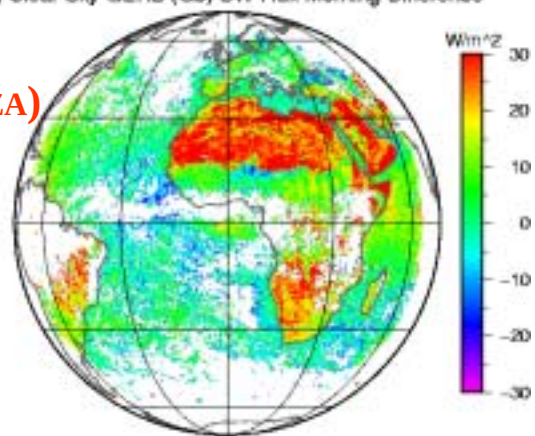

(B) Clear Sky GERB (G3) SW Flux Afternoon Difference

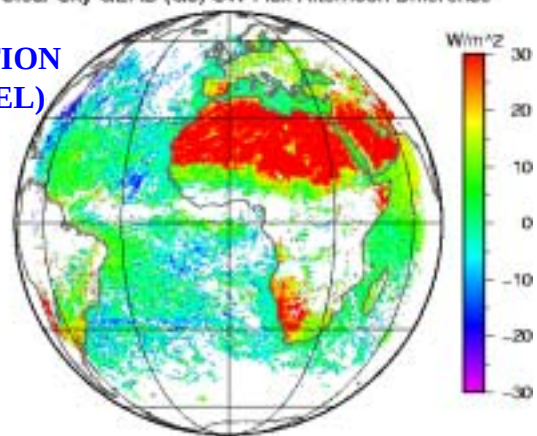

GERB

(C) Clear Sky GERB–like (S3) SW Flux Morning Difference

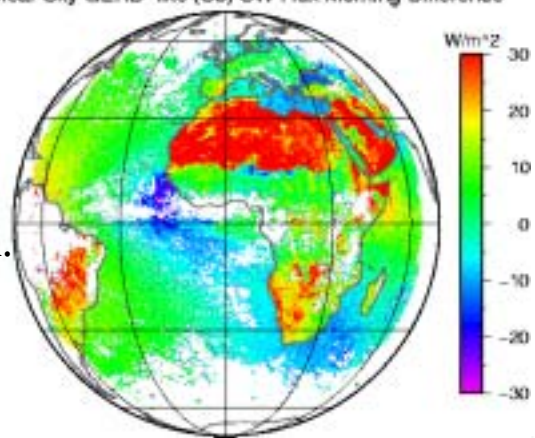

(D) Clear Sky GERB–like (S3) SW Flux Afternoon Difference

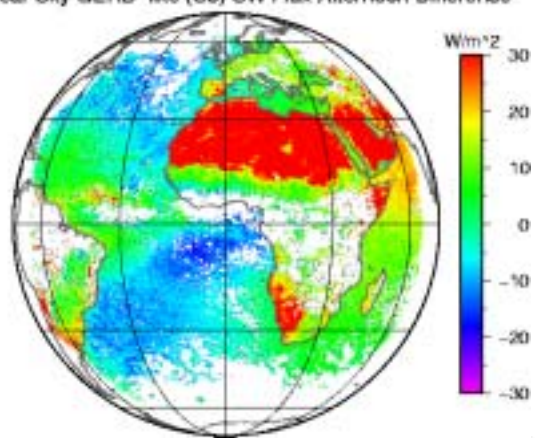

GERB-like
SEVIRI

<u>West</u>:
Max $F^{\uparrow}_{SW}$ after l.n.
⇒ positif ΔF
before l.n.

<u>East</u>:
Max $F^{\uparrow}_{SW}$
before l.n.
⇒ negatif ΔF
before l.n.

(E) Clear Sky CERES–TRMM ADMs SW Flux Morning Difference

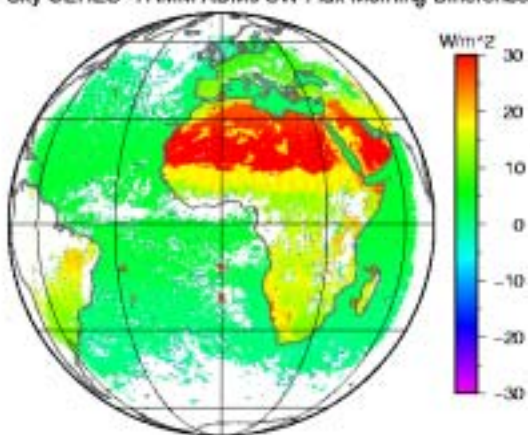

(F) Clear Sky CERES–TRMM ADMs SW Flux Afternoon Difference

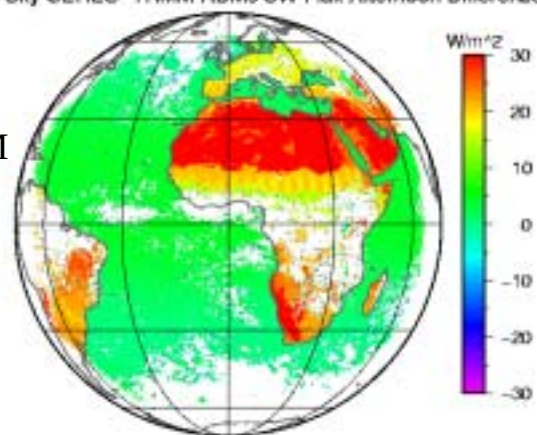

CERES-TRMM
ADM

Monthly Mean Diurnal Evolution (from sunrise to sunset)

Clear ocean GERB(-like) SW fluxes *(monthly mean data at the 3x3 SEVIRI pixel resolution -April 04-)*

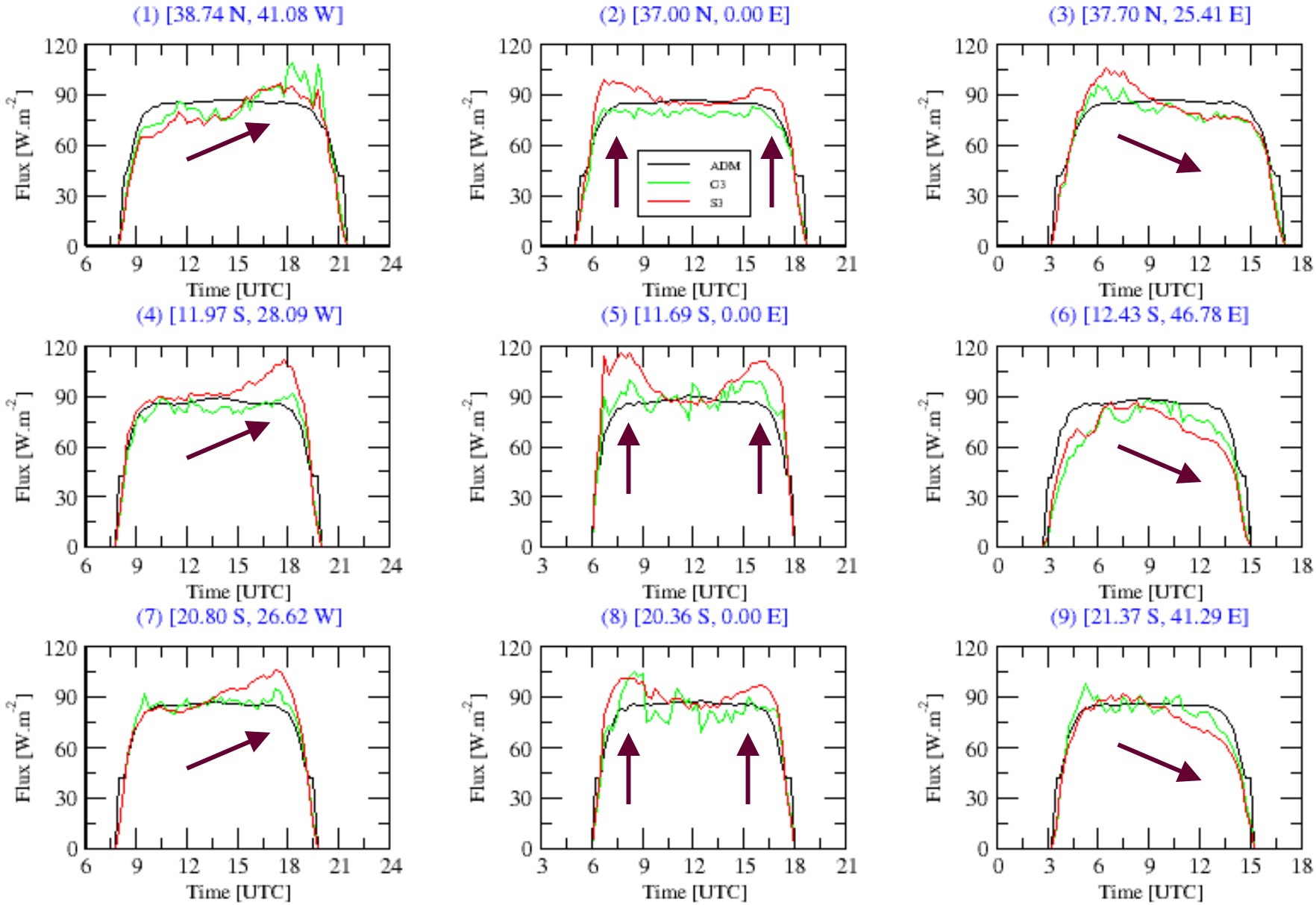

High frequency noise → cloud contamination

Selected ocean footprints (3x3 SEVIRI pixel resolution)

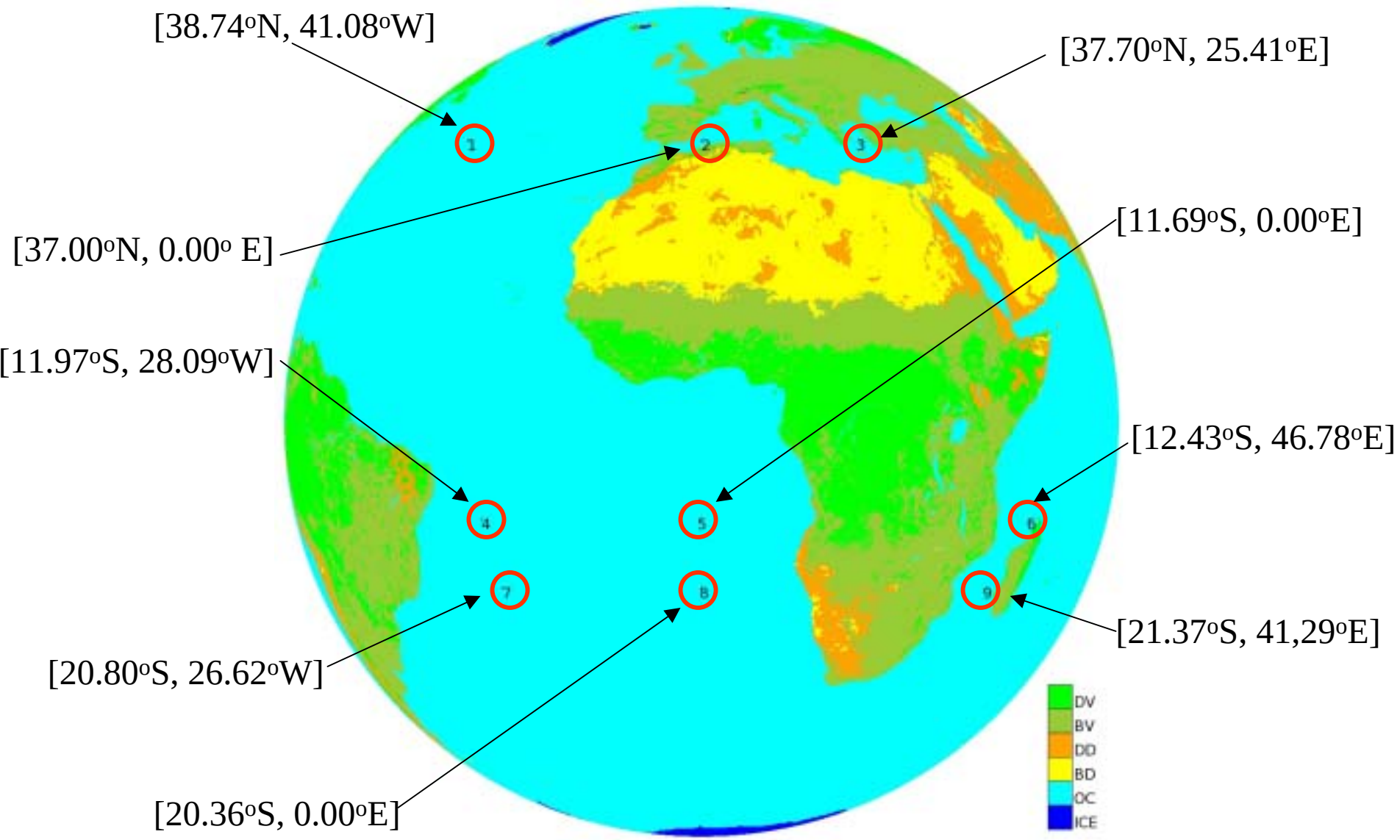

GERB unfiltering

SEVIRI NB measurements → spectral distribution of the observed radiation

$$L^{uf}_{GERB} = \left(\frac{L^{uf}_{SEVIRI}}{L^{f}_{SEVIRI}} \right) \cdot L^{f}_{GERB} = L^{uf}_{SEVIRI} \cdot \left(\frac{L^{f}_{GERB}}{L^{f}_{SEVIRI}} \right)$$

C = GERB corr. factor

α = SEVIRI unfilter factor

where

Spectral conversion: polynomial regression on the SEVIRI NB radiances

$$L^{f}_{SEVIRI} = a + b_1 L^{f}_{0.6} + b_2 L^{f}_{0.8} + b_3 L^{f}_{1.6} + c_{11} L^{f2}_{0.6} + c_{21} L^{f}_{0.8} L^{f}_{0.6} + c_{22} L^{f2}_{0.8} + c_{31} L^{f}_{1.6} L^{f}_{0.6} + c_{32} L^{f}_{1.6} L^{f}_{0.8} + c_{33} L^{f2}_{1.6}$$

$$L^{uf}_{SEVIRI} = a' + b_1' L^{f}_{0.6} + b_2' L^{f}_{0.8} + b_3' L^{f}_{1.6} + c_{11}' L^{f2}_{0.6} + c_{21} L^{f}_{0.8} L^{f}_{0.6} + c_{22}' L^{f2}_{0.8} + c_{31}' L^{f}_{1.6} L^{f}_{0.6} + c_{32}' L^{f}_{1.6} L^{f}_{0.8} + c_{33}' L^{f2}_{1.6}$$

- Data base of **theoretical** SBDART spectral **radiances** curves at TOA **assuming Lambertian surface reflectance**
- **Regression coefficients** evaluated for 10 SZA values **independent**ly of **surface type** and **cloud condition**

Radiance-to-flux conversion

Use of the CERES-TRMM BB SW ADMs

BUT: CERES footprint size on TRMM ≈ 10x10 km

Mean of 3x3 SEVIRI pixels SW radiances

(1) $$F_{3.SEVIRI}(\theta_{sm}) = \frac{\pi L^{uf}_{3.SEVIRI}(\theta_{sm},\theta_{vm},\phi_m)}{R_{adm}(\theta_{sm},\theta_{vm},\phi_m)}$$

Based on the average S.I.

(2) $$F_{GERB/3.SEVIRI}(\theta_{sm}) = F_{3.SEVIRI}(\theta_{sm}) * C_H(\theta_{sm},\theta_{vm},\phi_m)$$

GERB SW correction factor $\Rightarrow$ $L^f_{GERB/3.SEVIRI}$ / $L^f_{3.SEVIRI}$

Up-sampling of L^f_{GERB} from the nominal GERB footprint resolution to the high 3x3 SEVIRI pixel resolution

1. All Scenes [2004-04-25]

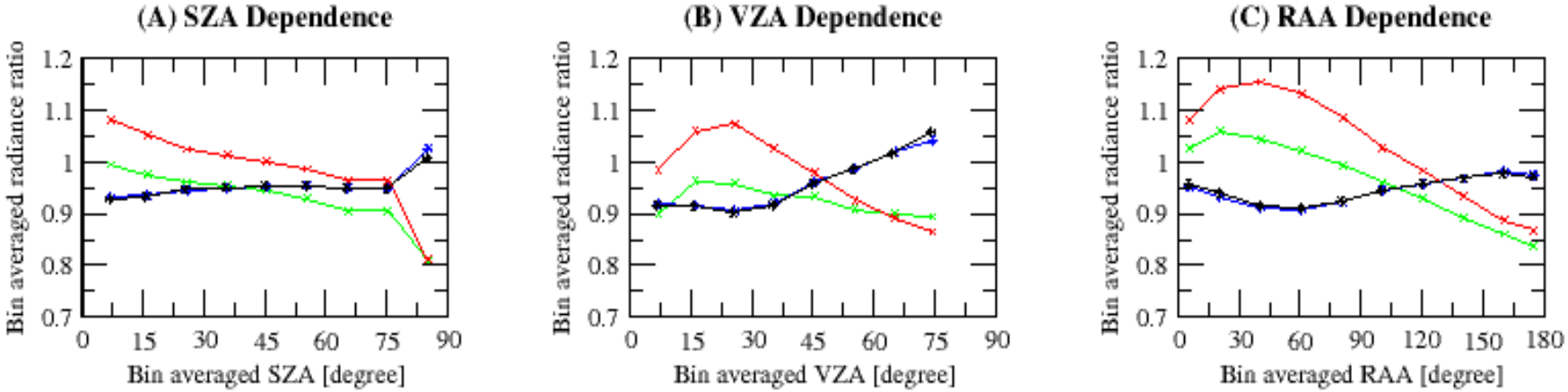

→ Good agreement between C_L and C_H when averaged over all scenes

2. Clear Ocean [2004-04-25]

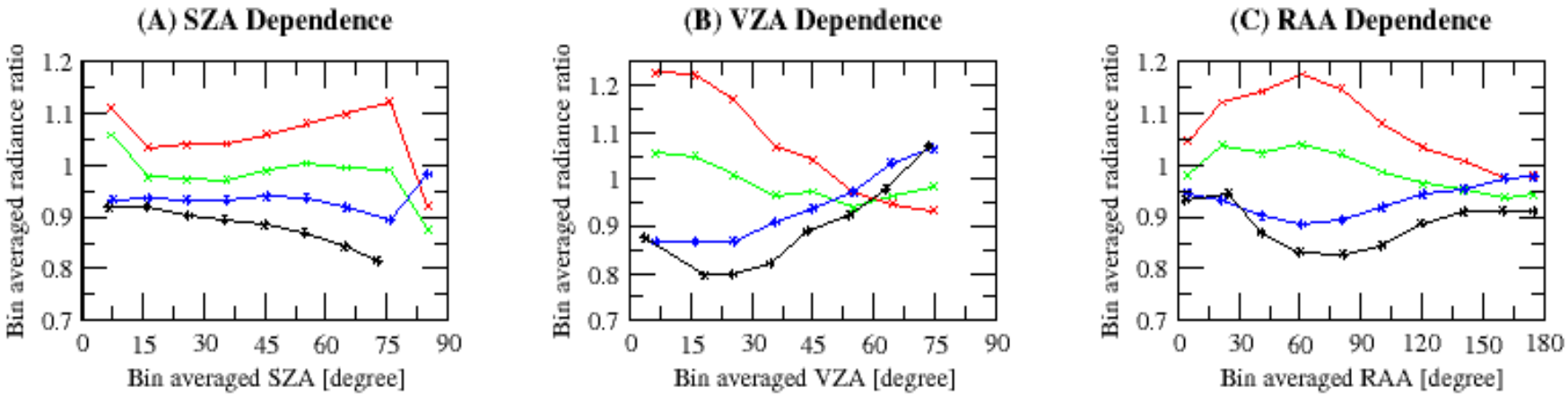

→ Asymmetry problem pointed out above clear ocean surface may still be serious in other scenes (single fit of coef, used for NB-to-BB conversion)

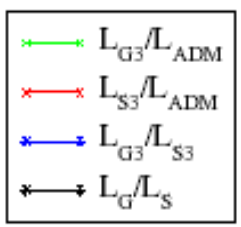

→ Correcting the SEVIRI based spectral modeling by GERB allows only part of the modeling errors to be removed

New Spectral Modeling

Empirical relations used:

Database of co-angular CERES and SEVIRI measurements (March, April and July 04 FM2/FM3 ES8 Edition 2 CERES data)

$$L^{uf}_{SEVIRI}\ (L^{uf}_{CERES} = \mathbf{c_0} + \mathbf{c_1}\, L^{f}_{0.6} + \mathbf{c_2}\, L^{f2}_{0.6} + \mathbf{c_3}\, L^{f}_{0.8} + \mathbf{c_4}\, L^{f}_{1.6} + \mathbf{c_5}\, SZA + \mathbf{c_6}\gamma$$

where c_i are **surface types dependent (**OC, DV, BV, DD, and BD**) but independent of the cloud condition !**

GLINT ANGLE

L^{f}_{SEVIRI} CAN NOT BE DETERMINED FROM CERES DATA

$$L^{f}_{SEVIRI,j} = L^{uf}_{SEVIRI,j} / \alpha_{th,j} \qquad (j=OC,DV,BV,or\ BD)$$

where α_{th} is a **theoretical unfilter factor** calculated from a database of theoretical spectral radiances (assuming Lambertian surface reflectance over ocean surface: Cox and Munck scheme)

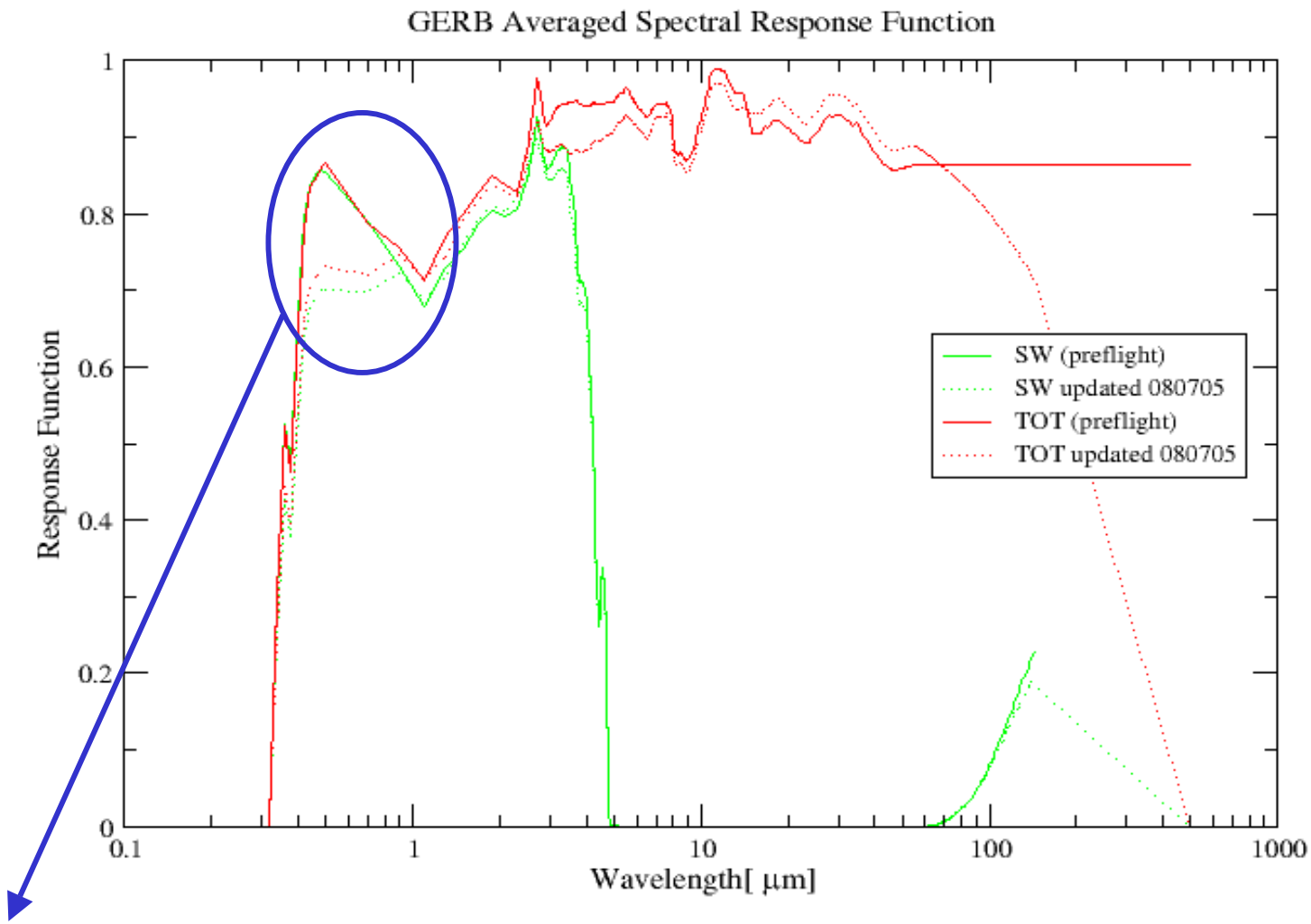

Adoption of the new response will ↑ GERB SW radiance

1. All Scenes [2006-01-15]

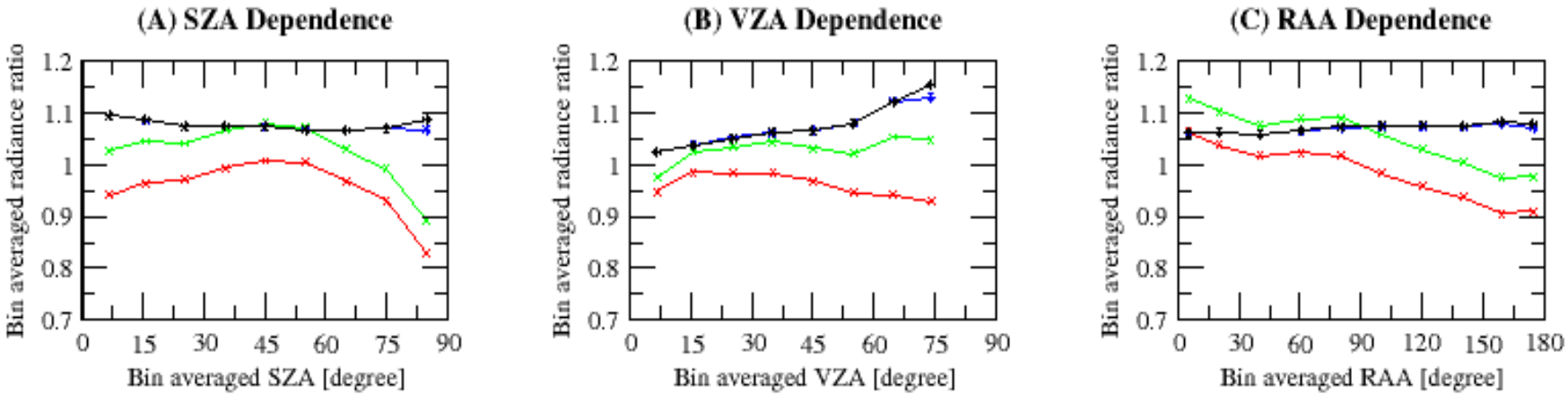

2. Clear Ocean [2006-01-15]

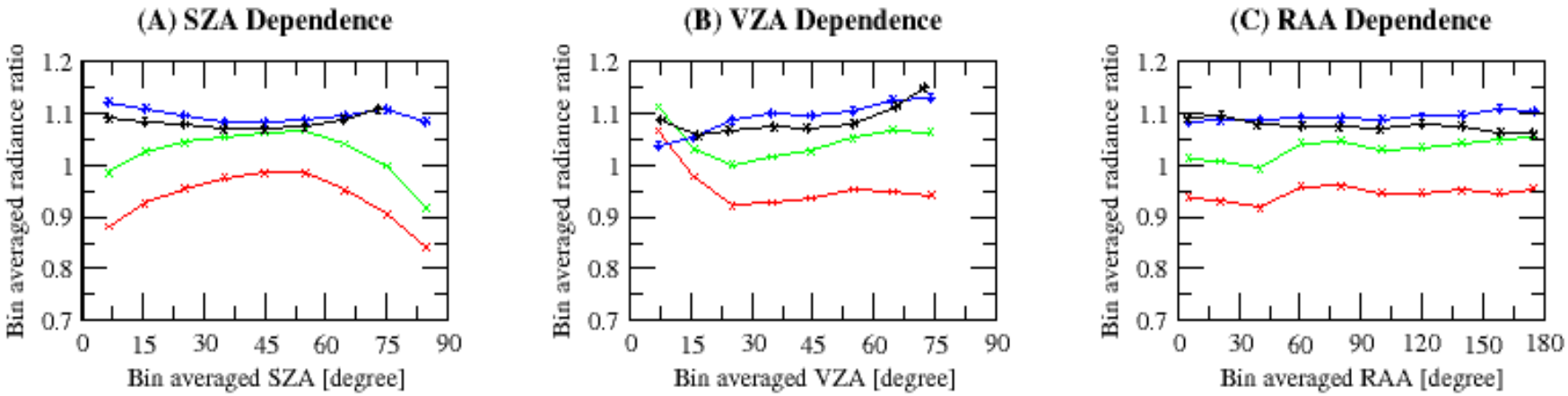

→ Angular dependence of C_L and C_H largely reduced excepted in VZA

→ Angular dependence in L_{S3}/L_{ADM}

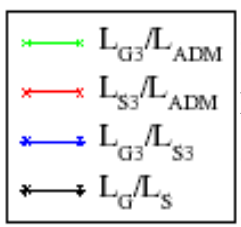

→ Correction of the SEVIRI based spectral modeling by GERB ↑ L^{uf}_{3S} by 8 to 10 %

→ Poor GERB correction: lack of function. of α_{th} with obs. angles and cloud condition

16 Days Mean Diurnal Evolution (from sunrise to sunset)

Clear ocean GERB(-like) SW fluxes *(16 days mean data at the 3x3 SEVIRI pixel resolution -16 to 31 January 06-)*

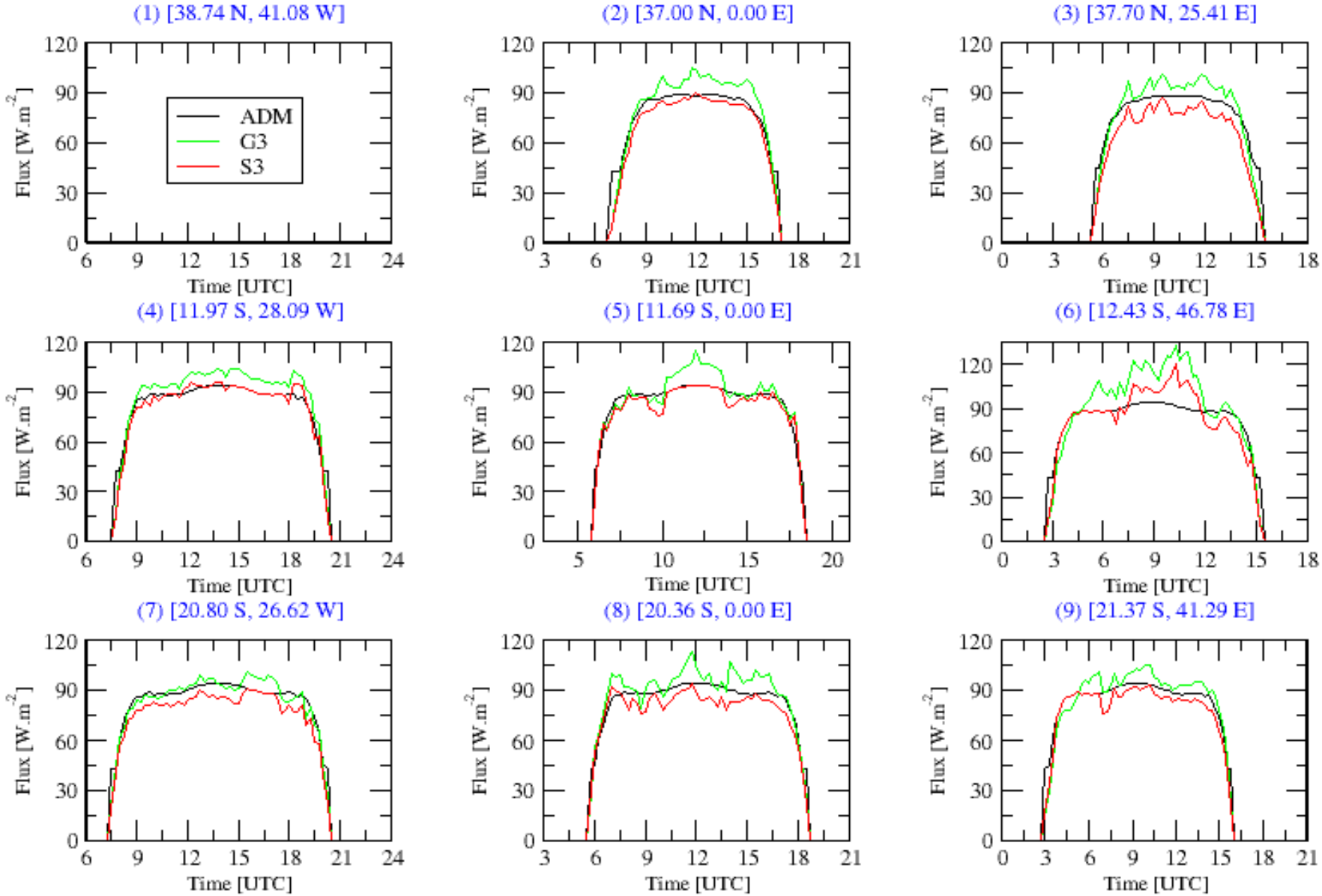

Conclusions

1. The primary cause of the asymmetry problem is the SEVIRI spectral modeling.
2. Empirically derived surface type dependent NB-to-BB equations have shown their usefulness in the reduction of the asymmetry problem.
3. Deficiencies in the cloud screening algorithm and hence in the scene identification essentially lead to add a high frequency variability (noise) in the GERB SW Flux time evolution.
4. The cloud contamination of c_H is more problematic as the efficiency of GERB in correcting the SEVIRI spectral modeling is reduced.

Resolution enhancement limitations:

- GERB and SEVIRI images recorded at ≠ times
  ⇒ temporal matching needed
- Scene types independent

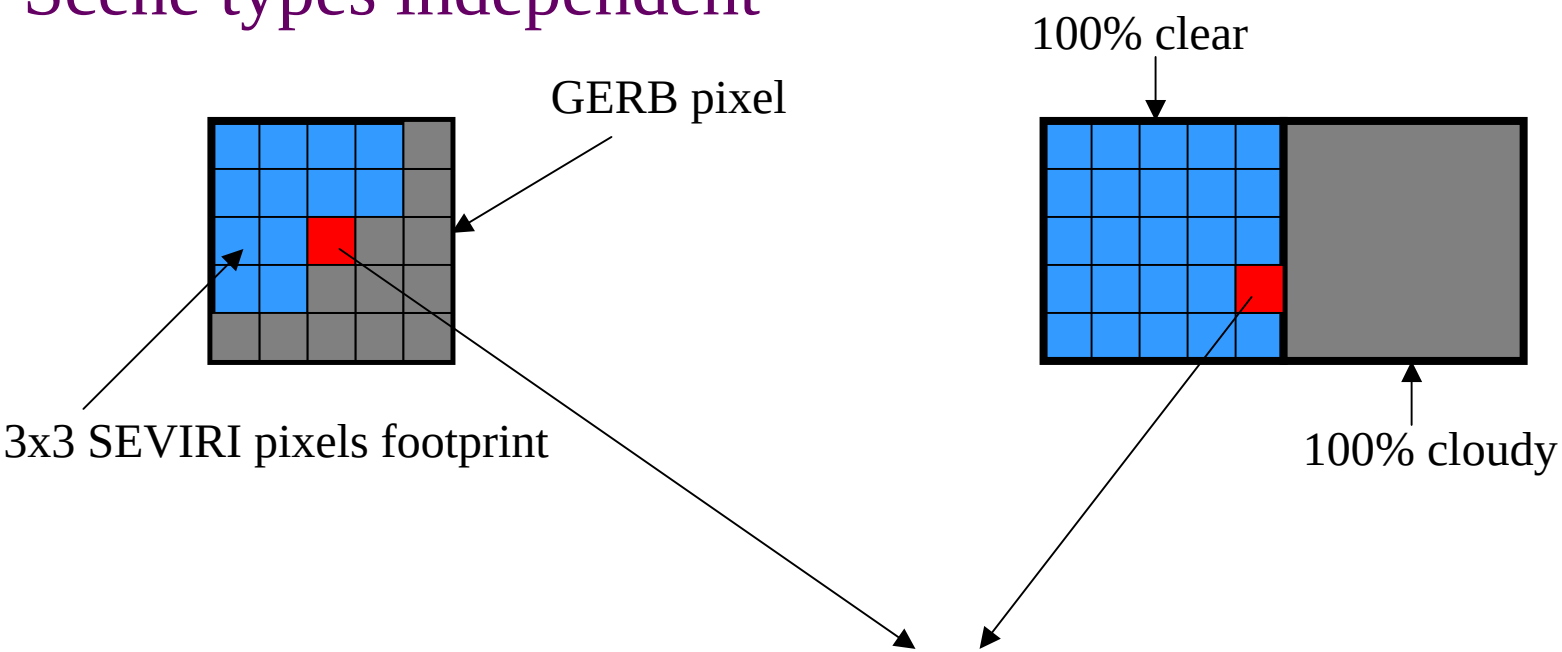

S3 footprint for which the $CF_H(x,y)$ will be cloud contaminated

Resolution enhancement (I)

Up-sampling of the filtered GERB radiances from the nominal GERB footprint resolution (i, j) to the 3 x 3 SEVIRI pixels resolution (x, y).

BUT: rather than L^{f}_{GERB} we use $CF = L^{f}_{GERB}/L^{f}_{SEVIRI}$

FIRST: Fluxes at the GERB footprint resolution (i, j) are derived from the 3 x 3 SEVIRI pixels (x, y) based flux estimates

$$F_{GERB}(i, j) = \left(\sum_x \sum_y PSF(i, j, x, y) \cdot F^{S3}(x, y)\right) . CF_L(i, j)$$

$$\Rightarrow CF_L(i, j) = \text{correction of SEVIRI by GERB}$$

SECOND: improvement of the spatial resolution of GERB fluxes by use of SEVIRI high resolution information

$$F_{GERB}(i, j) = \sum_x \sum_y PSF(i, j, x, y) \cdot CF_H(x, y) \cdot F^{S3}(x, y)$$

Resolution enhancement (II)

FINALLY: **GERB flux at the 3 x 3 SEVIRI pixels resolution is given by** $F^{G3}(x, y) = CF_H(x, y) \cdot F^{S3}(x, y)$

Clear ocean GERB(-like) TOA albedo *(monthly mean data at the 3x3 SEVIRI pixel resolution -April 04-)*

(1) [38.74 N, 41.08 W]

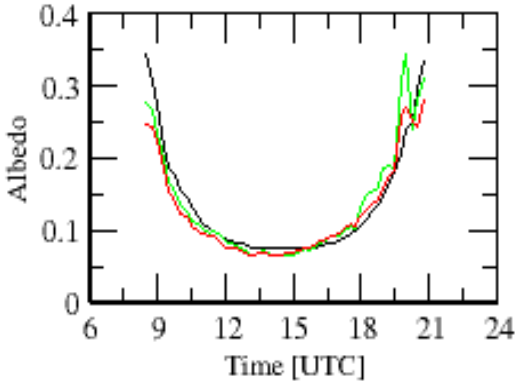

(2) [37.00 N, 0.00 E]

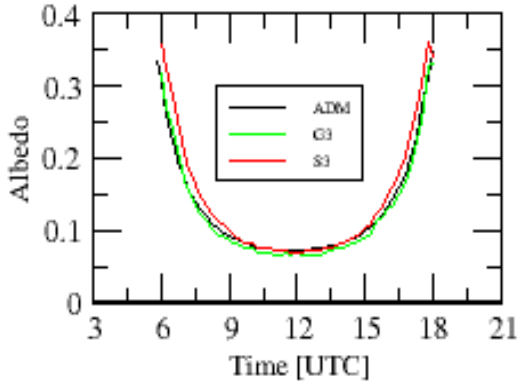

(3) [37.70 N, 25.41 E]

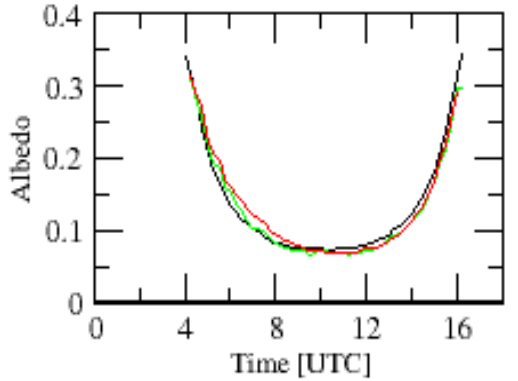

(4) [11.97 S, 28.09 W]

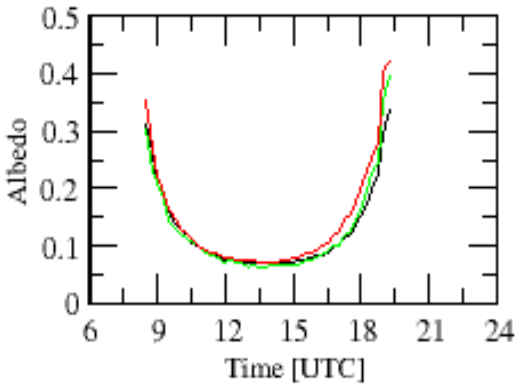

(5) [11.69 S, 0.00 E]

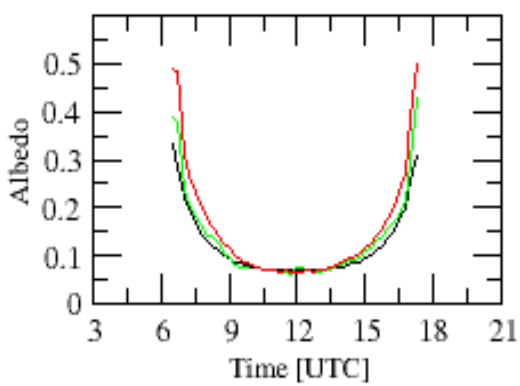

(6) [12.43 S, 46.78 E]

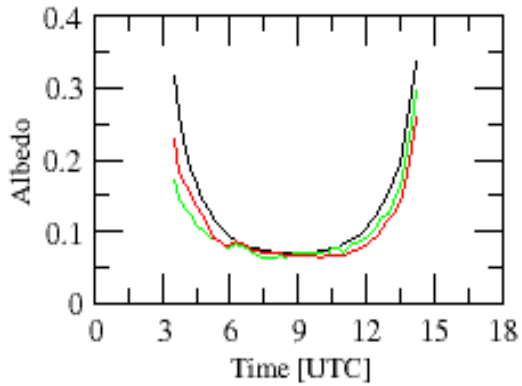

(7) [20.80 S, 26.62 W]

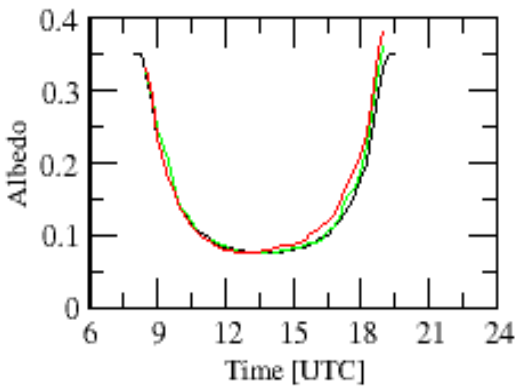

(8) [20.36 S, 0.00 E]

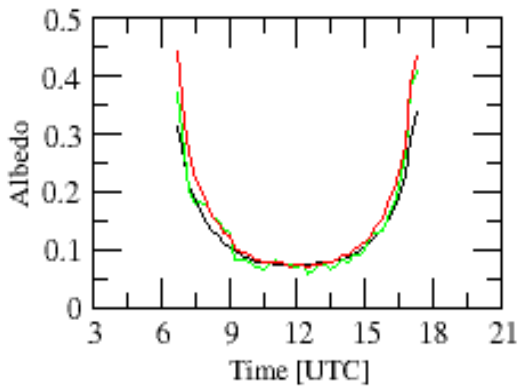

(9) [21.37 S, 41.29 E]

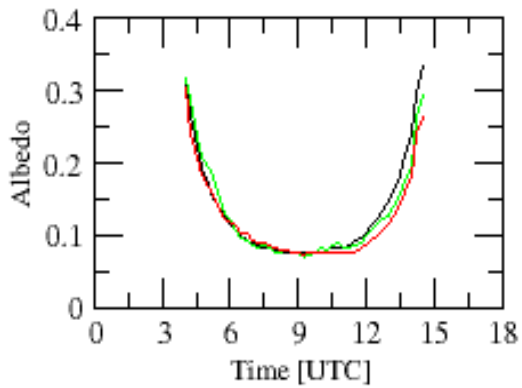

Clear ocean GERB(-like) SW radiances *(monthly mean data at the 3x3 SEVIRI pixel resolution -april 04-)*

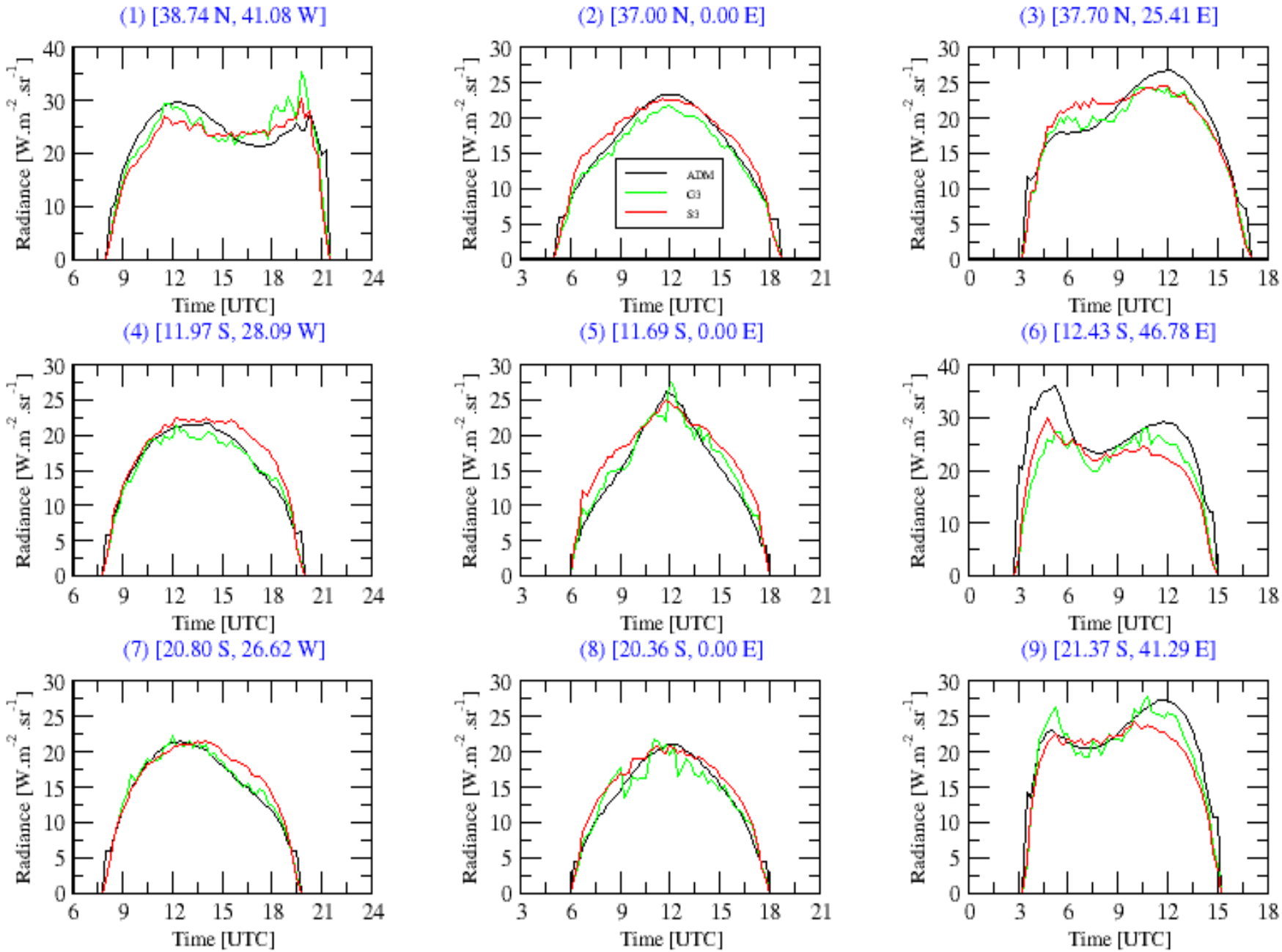

Clear ocean GERB(-like) TOA albedo *(16 days mean data at the 3x3 SEVIRI pixel resolution -16 to 31 January 06-)*

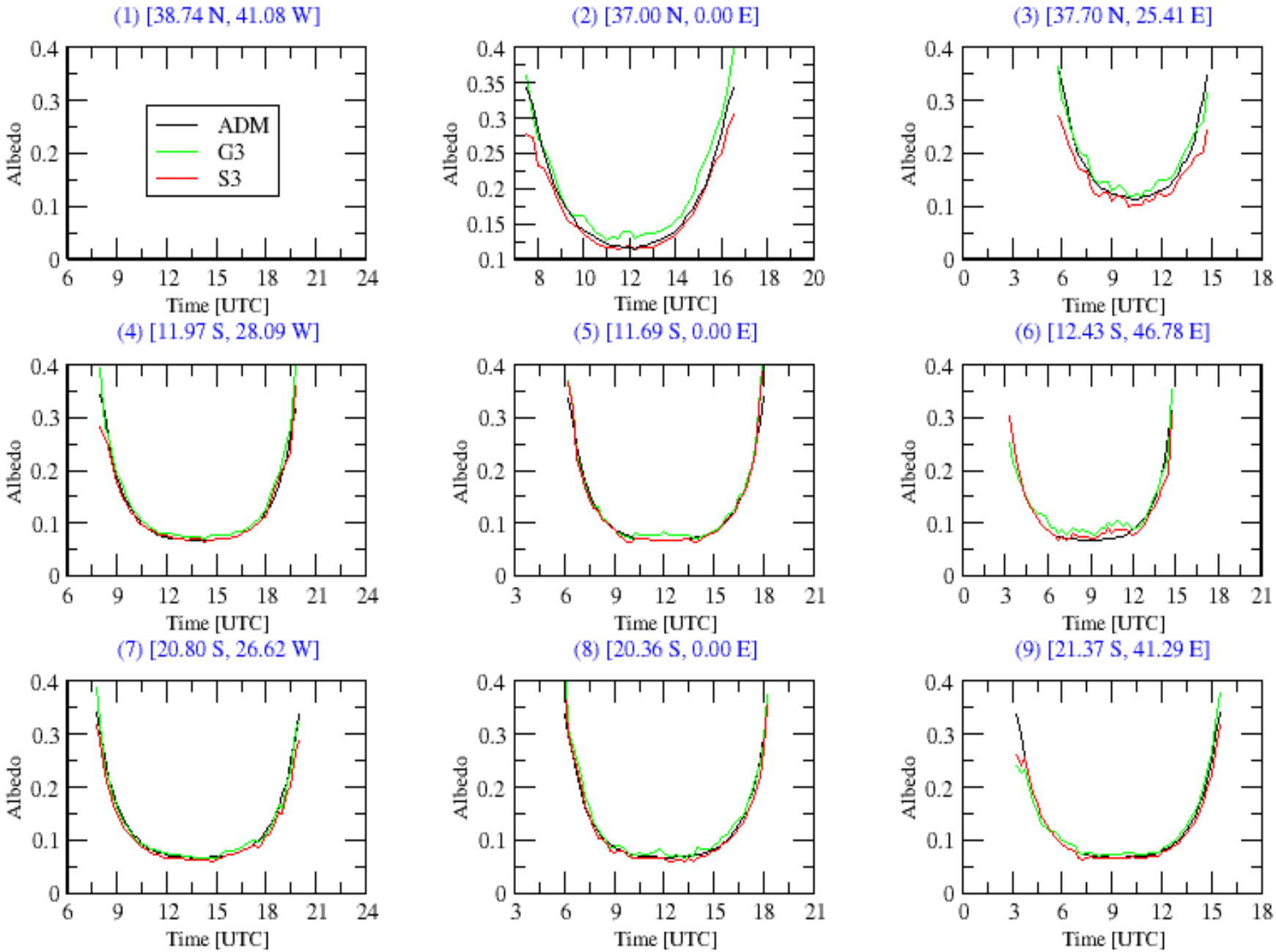

Clear ocean GERB(-like) SW radiances *(16 days mean data at the 3x3 SEVIRI pixel resolution -16 to 31 January 06-)*